TECHNISCHE UNIVERSITÄT BERLIN
Institut für Theoretische Physik
Prof. Dr. Holger Stark

Technische Universität Berlin

Control of Dynamic Wetting on Photo-Switchable Substrates

B – Project description

1 State of the art and preliminary work

1.0.1 State of the art

Photo-switchable substrates provide a unique mechanism to manipulate liquid droplets precisely by creating a light-induced wettability landscape, which changes in space and time. Because droplets respond to changes in the wettability of substrates, they can be kept out of equilibrium continuously, giving rise to new states of dynamic wetting. Substrate wettability determines the shape of the droplet contact line and contact angle, *i.e.* the geometry of its footprint. Changes in droplet shape, in turn, induce droplet motion as well as flow inside the droplet. This proposal plans to investigate the dynamic wetting behavior of droplets on photo-switchable substrates in response to external control *via* light, which in our theoretical approach means that wettability can be switched instantaneously.

Methods for driving droplets on complex substrates

Multiple methods to control dynamic wetting have been suggested and tested including thermal control based on the Leidenfrost effect [1], acoustic control using targeted substrate vibrations [2], and control of wettability, for example, through light-switchable coatings [3]. We briefly describe these systems.

The Leidenfrost effect refers to a liquid droplet floating above a hot surface from which it is separated by a layer of vapor. On a ratcheted surface it can be used to drive droplets in the geometrically prescribed direction [1]. Similarly, a heated surface covered with pillars of increasing width may be used to drive droplets in direction of increasing pillar width by inducing rotational flow inside the droplet [4].

Acoustic vibrations move droplets by transferring momentum from the substrate to the droplet and temporarily deforming it through “acoustic radiation pressure” [2], which originates from the vibrating substrate. In simulations, vibrations of the substrate combined with a pattern of stripes of high and low wettability and with increasing width, also induced directed motion of a liquid droplet [5].

Finally, methods of driving droplets make use of heterogeneous wettability caused by gradients in surface roughness [6], chemical composition [7], or temperature [8, 9]. For droplets on heterogeneous substrates with a static variation a hydrodynamic theory was first proposed in 1978 for the case of thin, viscous droplets [10]. Early experiments demonstrated that wettability gradients can be used to drive droplets towards higher wettability regions: A step-like increase in wettability draws droplets towards the side with higher wettability [11] while gradients of continuous wettability can drive droplets upwards against external forces [7]. Later experimental and simulation studies demonstrate trapping [12] and

driving [5, 13, 14] of droplets on substrates with checker-board, pillar, or stripe patterns, respectively.

The aim of our proposal is to study how droplets can be controlled by substrates with a spatio-temporal variation of wettability.

Theory of droplets on substrates with heterogeneous wettability

A thorough theoretical foundation exists to describe wetting on heterogeneous substrates. Here, we briefly summarize five important aspects of this fundamental research topic: Firstly, wetting under equilibrium conditions, where contact line and contact angle determine the droplet shape; secondly, hysteresis of the contact angle due to pinning of the contact line; thirdly, wetting under quasi-static conditions, where the droplet shape adjusts quasi instantaneously to the moving contact line and angle; fourthly, wetting under conditions of small contact angle such that droplet shape and internal flow fields are completely determined by the height profile of the droplet; and finally, the theoretical challenge of imposing appropriate boundary conditions for dynamic wetting in connection with the so-called *contact-line singularity*.

Equilibrium

Droplets in equilibrium minimize the sum of their surface energies from the gas and substrate interfaces, respectively, while conserving their volume [15]. If wetting is energetically more favorable than a dry substrate, the liquid phase covers the substrate with a thin film. Otherwise, a droplet forms with an energetically optimal ratio of the areas between liquid-gas and liquid-substrate interfaces. On homogeneous and planar substrates, the optimal shape obviously is a spherical cap. The force balance determines the contact angle θ of the circular three-phase contact line and results in Young's equation, which relates θ to the surface tensions γ_{ij} between liquid (l), gas (g), and substrate (s), respectively:

$$\gamma_{\mathrm{sg}} = \gamma_{\mathrm{sl}} + \gamma_{\mathrm{lg}} \cos(\theta) \ . \tag{1}$$

Higher wettability means smaller contact angle and according to Eq. (1) that the difference $\gamma_{\mathrm{sg}} - \gamma_{\mathrm{sl}}$ of both surface tensions at the substrate increases, since then it is energetically more favorable to cover the substrate with liquid. In our project, when we talk about dynamic wettability patterns, we will vary $\Delta\gamma_{\mathrm{s}} = \gamma_{\mathrm{sg}} - \gamma_{\mathrm{sl}}$ in time. On substrates with heterogeneous wettability the optimal droplet shape can be much more complicated including complex shapes of the contact line and varying curvature of the liquid-gas interface [16].

Ideal and non-ideal substrates, pinning

On an *ideal* substrate the contact angle always relaxes to its equilibrium value given by Young's equation. In contrast, on *non-ideal* substrates the contact line may be pinned at imperfections such that the contact angle of a receding or an advancing line remains below or above the equilibrium value, respectively. This phenomenon is called *contact angle hysteresis* (CAH) with a typical spread of contact angles of at least 5° [15]. The presence of CAH does not necessarily mean that a droplet keeps moving until its contact angles are equal. Instead it may stop with a slight imbalance between its advancing and receding side due to pinning. As a result, the equilibrium angle provides a useful approximation for the actual value of the contact angle but more detailed investigations must account for CAH. We describe our approach in Sec. 1.0.2. Recently, it was pointed out that CAH also exists while a droplet is dragged across a perfectly smooth surface due to energy dissipated in the flow field inside the droplet [17].

Quasi-static approach

Some theoretical studies have restricted themselves to a quasi-static approximation, where the droplet dynamics is fully described by the motion of the three-phase contact line. This is possible if the viscous time scale is much larger than the capillary time such that the free surface of the droplet relaxes so fast that it quasi instantaneously adjusts to the momentary

shape of the contact line. The quasi-static approach was applied to a droplet crossing a wettability step on a static substrate [16] and when calculating the friction forces of droplets with spherical caps [18, 19] or circular footprints [20]. However, since we plan to study how the droplet shape responds to a time-varying wettability with increasing rate, the quasi-static approach will only be applicable as a limiting case in our project.

Small-contact-angle approximation
In the small-contact-angle approximation the droplet shape is freely deformable under the constraint that the free surface can be parametrized by a height profile, which is a function of the coordinates in the substrate plane. This reduces the complexity of determining flow fields inside the droplet to dynamic equations of the height profile [21–23]. For example, this approach is able to accurately describe how droplets split after they have been placed on a stripe of low wettability [24, 25] as a comparison with experiments shows.[1] Because droplets require significant variation in contact angle to move, we will mainly use the full hydrodynamic Stokes equations instead.

Contact-line singularity
To this day, the dynamics of a droplet poses a significant theoretical challenge because the Stokes equations predict diverging energy dissipation for moving droplets due to an inherent contradiction. Conventionally, one imposes a no-slip boundary condition for fluid flow at a solid-liquid interface and, therefore, a contact line moving *on* the substrate is mathematically ill-defined [27]. Various approaches exist to address the issue, for example, by modifying the boundary conditions to allow some slip near the contact line (known as the *Navier condition*), by treating the contact line microscopically as a non-continuum problem, or by replacing the idealized sharp interface between liquid and gaseous phase with a diffuse transition region. All these approaches are reviewed in Ref. [15]. Because the contact-line singularity is not the focus of our project, we will use the Navier condition, which is an established approach.

Experiments with droplets on substrates with dynamic wettability

Several experiments have studied droplets moving on a substrate in response to *changing* wettability profiles. They are reviewed in Refs. [28, 29]. We mention them here and also provide real numbers for measured contact angles and droplet velocities.

On a substrate functionalized with light-switchable azobenzene, Ichimura *et al.* [3] first exposed a droplet to UV light with homogeneous intensity switching nearly all molecules into the cis state. Then, they partially switched the molecules back to the trans state by exposing the droplet to blue light with a gradient in intensity. This induced motion toward the region with lower intensity, where wettability obviously was higher. The droplet stopped when illuminating it uniformly with blue light. Similarly, exposing the droplet repeatedly to reversing gradients of UV and blue light induced an asymmetric spreading and directed drift motion of its center of mass. The authors further showed that contact angle and droplet velocity depended on the steepness of the intensity gradient with the contact angle varying between 11 and 24°and a peak velocity of roughly 60 μm/s for a 2 μl droplet.

Berná *et al.* studied droplets on a rotaxane-functionalized substrate and induced droplet motion by focusing a beam of UV light on one side of the droplet [30]. UV illumination reduced the contact angle from 35 to 13°and induced droplet motion at 11 μm/s on mica substrate. Similarly, Yang *et al.* moved droplets sitting on a substrate functionalized with azobenzene and were even able to merge two neighboring droplets [31]. The UV light reduced the advancing contact angle from 33 to 18°for a benzonitrile droplet, from 84 to 72°for a formamide droplet, and by 15°for a water droplet. We will draw on these results in

[1] Interestingly, stripes of low wettability can also be used to enhance coarsening of multiple small droplets into one larger droplet [26].

order to achieve a realistic dynamics of droplets in response to spatio-temporal wettability patterns.

Influence of evaporation and condensation on wetting

A liquid droplet evaporates molecules into an undersaturated gaseous phase, while oversaturation causes condensation on the droplet. These environmental conditions affect wetting because the total volume of liquid changes over time until liquid and gaseous phases are equilibrated. A better fundamental understanding of the involved processes is important for ink-based printing [32] and for efficient heat transfer when the gaseous phase or the substrate are either cooled or heated [33]. Dynamically changing wettability induces flow inside the droplets which affects condensation and evaporation. For example, during evaporation confined vortices form at specific contact angles inside the droplet [34], which can trap solutes and thereby guide their deposition. A similar mechanism for targeted deposition used Marangoni flow, which was induced by switching photoresponsive surfactants at the free droplet surface [35]. We will come back to these experiments in the next point.

In some applications, like cooling or dehumidification, it is important to quickly clear the substrate from condensing liquid and the resulting droplets, because otherwise they will form an isolating liquid layer between the solid surface and the gas phase [33]. Obviously, this reduces the performance of the appliance. One way to achieve this, is to drive droplets away using wettability gradients. However, due to pinning of the contact line (CAH), droplets can only move a short distance. In contrast, sharp light-induced gradients are a potential means to push droplets arbitrarily far by moving the wettability gradient along with the droplet. An alternative approach is realized in Ref. [36]. It first uses wettability gradients at the edge of wettability stripes to merge small droplets into larger ones. Then, as droplets become sufficiently large, they can drift away under gravity. Thus, wettability patterns are an adequate method to clear substrates from condensing droplets, which is important for enhancing the rate of cooling or dehumidification in appliances.

The aim of our proposal is to study how evaporation affects the motion of a droplet on substrates with dynamic wettability.

Printing by evaporation and light-driven deposition

When ink dries, dissolved molecules and colloids are deposited on the substrate in predictable non-uniform patters. Most often ring stains occur due to capillary flow [37]. After the *coffee ring effect* was first described, great effort has been made to suppress it using various approaches, since in many printing applications uniform deposition is needed. For example, the Marangoni effect can counteract capillary flows [38], and so can capillary forces themselves [39]. Later studies found that ellipsoidal particles deposit uniformly due to their shape [40] and that contact angle hysteresis is necessary to observe the coffee ring effect [41]. However, a more subtle control over deposition can also be achieved using photoresponsive surfactants on the droplet surface [35]. Inducing Marangoni flow by illumination with light, generates vortices inside the droplet. They trap solutes in specific parts of the droplet while it evaporates. This targeted deposition in patterns of sub-droplet size promises an even finer control in micro-printing applications.

Here, we propose to use photo-switchable substrates to initiate flow inside the droplet by a dynamically changing wettability and thereby control the deposition of solutes on the substrate during evaporation. Using the substrate to control flow has the advantage that surfactants will not contaminate the deposit.

Influence of external forces on wetting

External forces also influence dynamic wetting. For example, gravity changes contact angles by adding an energy cost depending on the local film thickness [42, 43]. This will also

affect the droplet motion on substrates with dynamic wettability. One can also consider the droplet with its footprint, the solid substrate, and a conducting plate below it forming a capacitor [44]. Applying an electric field across the substrate affects the contact angle similar to a change in liquid-substrate surface tension. In addition, electric stray fields at the contact line noticeably influence the nearby free surface of a small droplet and thereby its contact angle [44].

As long as external forces act normal to the substrate, they cannot induce additional droplet motion. Otherwise, they will influence the effect of wettability gradients; either enhancing or suppressing droplet motion. One important case are droplets sitting on an inclined substrate and driven upward by a wettability gradient [7].

In our planned research, we will study how external forces affect droplet motion due to dynamically changing wettability gradients.

Boundary element method

We plan to employ the *boundary element method* (BEM) for the numerical parts of our project. The BEM uses Green's formalism to find solutions to linear partial differential equations based on an implicit integral equation for the field variables. Typically, Green's functions of partial differential equations are well-known for the unbounded space but unknown for geometries with specific boundaries. In such cases, one can either find a specialized Green's function for the given geometry (for example through the *method of mirror charges*) or formulate the implicit integral equation, which only contains integrals over the boundary of the integration volume. The BEM follows the latter approach and first solves the integral equation on this boundary using appropriate boundary conditions [45]. This is done on a spatially discretized mesh. Accordingly, the choice of mesh and the specific algorithm for determining the field variables on the boundary characterizes the BEM. We will describe the method applied to Stokes flow in a moving droplet in more detail in Sec. 1.0.2.

One important challenge the BEM faces are the singularities that Green's functions often contain. To accurately approximate the boundary conditions, Green's functions and their singularities need to be calculated on the domain boundary. This is usually done by separating singular and non-singular integrals and using analytical methods to handle any singularity contained in Green's function before numerical computations start (see, *e.g.*, Refs. [46, 47]). Alternatively, some numerical integration packages are able to automatically calculate singular integrals as long as the singularity is on the edge of the integration region (see, *e.g.*, the *Gauss-Kronrod method* in Ref. [48]).

Another challenge specific to Stokes flow is mass conservation. While the exact solution given by the Oseen tensor (Green's function of the Stokes equations) conserves mass, the same is not true for numerical solutions, since they can only provide approximate flow fields. Recently, Alinovi *et al.* proposed an extended BEM, which enforces mass conservation by adding an explicit side condition and a corresponding vector of Lagrange multipliers [47].

In our project we will use openly available algorithms and computer programs to develop a BEM suitable to describe droplets moving on substrate with switchable wettability.

1.0.2 Preliminary work

The group of the applicant has extensive experience with hydrodynamics at low Reynolds numbers as exemplified by a recent review on microswimmers [49]. It has also worked with photo-switchable molecules either tethered to a solid substrate [50] or as surfactants on curved [51] and planar [52] fluid interfaces. Especially the experience gained in self-consistently solving the Stokes equations for the flow field coupled to the surfactant dynamics at an interface will help us in addressing the problems formulated in this proposal.

We shortly review this work and then our preliminary work towards formulating the BEM for droplets on switchable substrates.

Collective dynamics of photo-switchable molecules

The dynamics of wetting is fundamentally linked to the dynamics of the substrate, especially for photo-switchable substrates. Many photo-switchable substrates are covered with compounds containing the azobenzene group, which changes its configuration (trans/cis) when exposed to either blue or UV light [28, 29]. We recently studied the dynamics of dry substrates with a monolayer of model molecules tethered to the surface. The model molecules were needles with a simplified overlap interaction, which change their shape between straight and bent at rates proportional to light intensity [50]. In kinetic Monte Carlo simulations without switching we found that initial nematic order of straight needles decays in time like a power law for strong overlap interactions, which indicates glass-like dynamics. The slow relaxation can efficiently be controlled and accelerated by illuminating the monolayer with circularly polarized light, which induces trans-cis isomerization cycles. Thus, pushing the substrate out of equilibrium creates new relaxational dynamics.

Photoresponsive fluid interfaces

Closely related to wetting on photo-switchable substrates is the dynamics of photoresponsive fluid interfaces, where light-switchable surfactants are placed at the boundaries between two immiscible fluids. Many such molecules exist based on stereoisomeric groups, including azobenzene and spiropyran [29]. Locally switching between surfactant isomers induces a gradient in surface tension along the interface, which drives Marangoni flow [53].

Recently, we have determined the full analytic solution for the flow field inside and outside of an emulsion droplet created by an arbitrary surface tension field at its interface. Combined with a diffusion-reaction-advection equation for the order parameter of the surfactant mixture [54, 55], we showed that a single light beam can drive an oil droplet (covered by a photo-switchable surfactant) either towards the light source or away from it. The droplet thereby performs transverse oscillations about the light beam [51]. Recent experiments demonstrated the motion of emulsion droplets induced by light [56, 57].

Extending our theory for the surfactant mixture, we have also studied the situation, where light spots on planar fluid interfaces are switched on and off [52]. Notably, implementing a nonlocal feedback between the induced Marangoni flow and the light intensity creates regular or irregular oscillations in polygons with an even or uneven number of light spots, respectively.

Boundary element method for droplets on switchable substrates

The theory outlined in this section forms the basis for the planned numerical investigations.

The boundary element method (BEM) approximates solutions to linear partial differential equations (PDEs) based on their Green's functions. For droplets moving on substrates, we need to study Stokes flow in incompressible fluids, which obeys two linear PDEs for velocity $\boldsymbol{v}$ and pressure p,

$$\mu \nabla^2 \boldsymbol{v}(\boldsymbol{r}) = \nabla p(\boldsymbol{r}) \quad \text{and} \quad \nabla \cdot \boldsymbol{v}(\boldsymbol{r}) = 0\,, \tag{2}$$

where μ is the shear viscosity and $\boldsymbol{r}$ the position vector. Green's function for Stokes flow in $\mathbb{R}^3$ is the Oseen tensor

$$\mathbf{O}(\boldsymbol{r}) = \frac{1}{8\pi\mu|\boldsymbol{r}|}\left(\mathbf{1} - \frac{\boldsymbol{r}\otimes\boldsymbol{r}}{|\boldsymbol{r}|^2}\right)\,. \tag{3}$$

We are interested in the flow field inside the closed volume of a droplet. On any compact region $D \subset \mathbb{R}^3$ with boundary ∂D and outward normal described by unit vector $\boldsymbol{n}$, it fulfills

the following integral equation [45, 58, 59]:

$$f(\boldsymbol{r})\boldsymbol{v}(\boldsymbol{r}) = \oint_{\partial D} \mathbf{O}(\boldsymbol{r}-\boldsymbol{r}')\boldsymbol{\Sigma}(\boldsymbol{r}')\boldsymbol{n}(\boldsymbol{r}')\,\mathrm{d}^2\boldsymbol{r}' - \oint_{\partial D} \boldsymbol{v}(\boldsymbol{r}')\cdot\mathbf{S}(\boldsymbol{r}-\boldsymbol{r}')\boldsymbol{n}(\boldsymbol{r}')\,\mathrm{d}^2\boldsymbol{r}' \,. \tag{4}$$

Here, $\boldsymbol{\Sigma}$ is the stress tensor of the fluid, $\mathbf{S}$ is the stress field of $\mathbf{O}$, and $f(\boldsymbol{r})$ is a dimensionless coefficient, which assumes different values inside and at the boundary of D [59]:

$$f(\boldsymbol{r}) = \begin{cases} 1 & \text{for } \boldsymbol{r} \in D \setminus \partial D \\ \frac{1}{2} & \text{for } \boldsymbol{r} \in \partial D, \text{ where } \partial D \text{ is smooth} \\ \frac{\alpha}{4\pi} & \text{for } \boldsymbol{r} \in \partial D, \text{ where } \partial D \text{ has a corner with inward solid angle } \alpha \end{cases} . \tag{5}$$

Although the integral equation is closed (because it only depends on $\boldsymbol{v}$), it is also implicit because $\boldsymbol{v}$ appears on both sides. The BEM discretizes the integrals in the integral equation so that approximate values for $\boldsymbol{v}$ can be calculated on each piece of ∂D and, thereafter, anywhere on D. Determining the field variable on the interface is the main challenge inherent in any BEM [46].

A droplet with a "free" (meaning movable) surface raises several challenges for a numerical solution of the integral equation. Firstly, the droplet boundary consists of two parts, one interface with a solid substrate and a second with a gas phase. This means each part has its own boundary condition. At the interface with the substrate there is a Robin boundary condition (for fluids called the Navier condition), $\mu\boldsymbol{v} + \lambda\boldsymbol{\Sigma}\boldsymbol{n} = 0$ with a possible slip length λ, which connects velocity and normal stress. A typical value for the slip length is $\lambda \approx 1\,\mathrm{nm}$ [15]. At the interface towards the gas phase we assume zero viscosity of the gas phase so that the tangential stress is zero. There remains a Neumann boundary condition (in hydrostatics the Laplace pressure), $\boldsymbol{n}\cdot\boldsymbol{\Sigma}\boldsymbol{n} = -2\gamma\kappa$, which locally relates the normal stress component $\boldsymbol{n}\cdot\boldsymbol{\Sigma}\boldsymbol{n}$ to the mean curvature κ, where γ is the local surface tension. To solve the integral equation, we need to first calculate $\boldsymbol{v}$ on the free and substrate surfaces by inserting the boundary conditions and inverting the resulting equation. This is done by discretizing each surface with many small elements with constant values for $\boldsymbol{v}$ on each piece. This converts the integral equation into a system of linear equations, where the missing values for $\boldsymbol{v}$ form a vector of unknowns and the piece-wise integrals determine the elements of a matrix operating on this vector [47]. By applying standard matrix inversion methods, the linear problem yields approximations for $\boldsymbol{v}$ anywhere on the boundary. Once these quantities are known, $\boldsymbol{v}(\boldsymbol{r})$ can be calculated anywhere by straightforward integration.

The second challenge is the dynamics of the free surface specified by the position vector $\boldsymbol{s}$. It moves locally with the normal component of the fluid velocity,

$$\frac{\partial \boldsymbol{s}}{\partial t} = [\boldsymbol{n}(\boldsymbol{s}) \otimes \boldsymbol{n}(\boldsymbol{s})]\boldsymbol{v}(\boldsymbol{s}) \,. \tag{6}$$

Finally, the contact angle must be specified. Young's law stated in Eq. (1) is inadequate because it does not account for pinning and friction of the contact line (CAH) [15]. However, several approximate corrections for Young's law exist, which are used for dynamic wetting [15, 60–62]. The most well-known among them is the Cox-Voinov law [63, 64] derived from hydrodynamic considerations:

$$\theta_{\mathrm{dyn}}^3 = \theta_{\mathrm{micro}}^3 + A v_{\mathrm{contact}} \tag{7}$$

It relates the dynamic and microscopic contact angles, θ_{dyn} and θ_{micro}, taking into account the velocity of the contact line v_{contact}. The coefficient A is determined completely by the slip length and the material properties of the liquid phase. The microscopic angle θ_{micro} is assumed to follow Young's law [62] and the velocity of the contact line is given by the fluid

velocity perpendicular to the contact line in the plane of the substrate. We impose θ_{dyn} as a boundary condition on the surface normal $\boldsymbol{n}$ at the contact line:

$$\boldsymbol{n}(\boldsymbol{c}, t) \cdot \boldsymbol{e}_z = \cos\theta_{\text{dyn}} \,. \tag{8}$$

On a light-switchable substrate the light patterns affect the surface tension difference $\Delta\gamma_{\text{s}} = \gamma_{\text{sg}} - \gamma_{\text{sl}}$ in Eq. (1). Therefore, as mentioned already, we will treat $\Delta\gamma_{\text{s}}$ as a heterogeneous and dynamic quantity, which determines θ_{micro} and, thereby, affects the shape of the droplet. Note that time appears through the equation for the droplet surface $\boldsymbol{s}$ in our problem, to which the Stokes flow adapts instantaneously. Numerically, the dynamics of $\boldsymbol{s}$ can be calculated using a standard Runge-Kutta algorithm in combination with the BEM described above.

1.1 Project-related publications

1.1.1 Articles published by outlets with scientific quality assurance, book publications, and works accepted for publication but not yet published

1. J. Grawitter and H. Stark, *Feedback-control of photoresponsive fluid interfaces*, Soft Matter **14**, 1856 (2018).

2. M. Schmitt and H. Stark, *Marangoni flow at droplet interfaces: Three-dimensional solution and applications*, Phys. Fluids **28**, 012106 (2016).

3. R. Tavarone, P. Charbonneau, and H. Stark, *Kinetic Monte Carlo simulations for birefringence relaxation of photo-switchable molecules on a surface*, J. Chem. Phys. **144**, 104703 (2016).

4. M. Schmitt and H. Stark, *Active Brownian motion of emulsion droplets: Coarsening dynamics at the interface and rotational diffusion*, Eur. Phys. J. E **39**, 80 (2016).

5. A. Pototsky, U. Thiele, and H. Stark, *Mode instabilities and dynamic patterns in a colony of self-propelled surfactant particles covering a thin liquid layer*, Eur. Phys. J. E **39**, 51 (2016).

6. A. Zöttl and H. Stark, *Emergent behavior in active colloids*, J. Phys.: Condens. Matter **28**, 253001 (2016).

7. R. Tavarone, P. Charbonneau, and H. Stark, *Phase ordering of zig-zag and bow-shaped hard needles in two dimensions*, J. Chem. Phys. **143**, 114505 (2015).

8. A. Pototsky, U. Thiele, and H. Stark, *Stability of liquid films covered by a carpet of self-propelled surfactant particles*, Phys. Rev. E **90**, 030401(R) (2014).

9. M. Schmitt and H. Stark, *Swimming active droplet: A theoretical analysis*, EPL **101**, 44008 (2013).

10. P. Kählitz, M. Schoen, and H. Stark, *Clustering and mobility of hard rods in a quasicrystalline substrate potential*, J. Chem. Phys. **137**, 224705 (2012).

1.1.2 Other publications —

1.1.3 Patents —

2 Objectives and work program

2.1 Anticipated total duration of the project

The project is intended to last for the whole duration of the priority program, *i.e.* for 6 years.

With the current proposal funding is requested for 36 months starting on 01. 10. 2019 or earlier.

2.2 Objectives

The central aim of our proposal is to move beyond static wetting and focus on substrates with switchable wettability that can be controlled dynamically. In particular, we have photo-switchable substrates in mind, which change their wetting properties quasi instantaneously in response to light. This will enable us to explore the coupled and highly complex dynamics of droplet motion and substrate wettability. Thereby, we will also develop the fundamental understanding for future applications, for example, in printing [32] or cooling/dehumidification devices [33].

Our investigation will be based on analytical arguments and numerical calculations, using the boundary element method (BEM) for low Reynolds number hydrodynamics (Stokes flow). Our first objective will be to fully implement the BEM in order to determine the Stokes flow inside a deforming liquid droplet that moves on a substrate with switchable wettability. Our analytical and numerical methods will cover a number of adjustable parameters: droplet volume, equilibrium contact angles, contact angle hysteresis, and slip length. We will explore the effect of different spatio-temporal wettability patterns by varying the strength of gradients or the amplitudes and frequencies of oscillations. For each study within the project we will focus on specific parameters to address the relevant research questions.

In the second objective we will investigate how droplets respond to specific spatio-temporal wettability patterns that either move or deform the droplet. To generate directed motion, we will test traveling patterns passing beneath the droplet either with a step-like increase in wettability or a plane-wave modulation. In both cases we are interested in optimal parameters, which maximize droplet speed, *i.e.*, velocity and amplitude of the pattern, and wavelength of the planar wave. To deform the droplet, we will test oscillating and rotating wettability patterns that vary along the contact line according to different angular harmonics. For both parts, we will closely observe the internal flow fields of the droplet to gain a deeper understanding of its response. Besides referring to literature, we will also use realistic values of dynamic contact angles provided by the project of **R. Haag** (FU Berlin) and information for the substrate surface tensions provided by the project of **E. Backus/M. Bonn** (MPI Mainz). We will also collaborate with the project of **S. Santer**(Potsdam), which can explicitly generate dynamic wettability patterns.

In the third objective we will investigate how condensation and evaporation affects the response of droplets to dynamic wettability patterns, *i.e.*, when the droplets grow or shrink. Because the shape is driven out of equilibrium both through dynamic wettability and volume changes, we expect complex interactions w.r.t. the internal flow. This is especially relevant during evaporation, where vortices in the internal flow field can trap and isolate solutes in some parts of the droplet [34, 35] and thereby determine where they are deposited.

In the fourth objective we will investigate how droplets respond to dynamic wettability in the presence of gravitational or electrostatic forces. These body forces compete with surface tension to determine the droplet shape and thereby influence how the droplet reacts in and out of equilibrium. Specifically, we will take the spatio-temporal wettability patterns from the first part and study how external forces modify both the optimal patterns to move the droplet and the dynamics of the droplet deformations. In addition, we will also investigate if and how dynamic wettability patterns can stabilize droplets against external forces. For example, can such patterns prevent a droplet from running down an inclined plate. The combination of external forces and dynamic wettability is important for many practical situations such as cooling systems or dehumidification.

Finally, in addition to investigating dynamic wettability patterns, we will also consider a simple approach to rough substrates by describing them with a non-zero slip length at the fluid/substrate interface. This directly connects to the project of **R. Haag** (FU Berlin), which is also concerned with dynamic wetting on rough surfaces.

Based on the objectives just formulated, the resulting steps of our work program can be summarized as follows:

1. Numerical computation of droplet dynamics
   Implement a boundary element method to describe a droplet with moving contact line and varying shape for relevant parameters.

2. Moving and deforming droplets using dynamic wettability patterns
   What are optimal patterns for droplet speed? What are the insights from internal flow fields?

3. Driving condensing and evaporating droplets
   Interaction with dynamic wettability, control of solute deposition.

4. External forces acting on driven droplets
   Influence of gravity and electrostatic forces on moving and deforming droplets.

5. Dynamic wetting on rough substrates
   Simple approach through a non-zero slip length at the liquid/substrate interface.

Besides the research program formulated by the objectives and collaborations mentioned in the work program, we are open to collaborate with other groups within the priority program by providing theoretical support for problems, which will come up during their research work. In particular, the numerical computation of droplet dynamics, which we will implement based on the BEM, will serve as a versatile tool to support experimental projects within the priority program or to compare to alternative computational approaches within the SPP.

We now introduce the individual steps of our work program in more detail.

2.3 Work program incl. proposed research methods

1. Numerical computation of droplet dynamics

As a prerequisite for our detailed studies, we will set up the necessary computer program to self-consistently determine the Stokes flow inside the droplet together with the dynamically varying free surface and contact line of the droplet. To start, we will take cue from *BEMLIB*, an instructional implementation of the boundary element method for Stokes flow [59], and more recent progress in computational physics [46, 47, 65, 66]. *BEMLIB* already supports simulations of *pinned* droplets on a substrate with an external flow streaming past the

droplet [67]. However, our studies require a more versatile program, which is able to describe changing droplet shapes and moving contact lines with varying contact angle along the line. We will use *BEMLIB* to produce reference data and validate our simulations.

The basic theory for formulating a BEM for moving droplets has already been described at the end of our preliminary work in Sec. 1.0.2. A main point is to choose an appropriate discretization and parameterization for the free surface and substrate surface, and to implement the necessary boundary conditions. The discretization describes the surface and is used to approximately calculate unknown boundary values for normal stress and velocity, which appear in the imposed boundary conditions. At the liquid-gas interface (*free surface*) the normal stress is known through the mean curvature of the surface and velocity is unknown. At the liquid-substrate interface a linear combination of normal stress and velocity is known, which can be used to eliminate either quantity from Eq. (4) and solve for the remaining quantity.

In BEMs the discretization consists of a mesh of points, which describes the location of each interface in space. To approximate surface integrals, the mesh has to be sufficiently fine-meshed and appropriately parameterized to allow calculating local curvature, normal vector, and the area associated with each discrete element. Because the mesh changes as the droplet moves and deforms, these quantities need to be calculated repeatedly and efficiently – a task which is well-suited for parallel computation. In our implementation, we will build upon existing numerical codes from open-source libraries as much as possible; especially w.r.t. algorithms for automatic differentiation, quadrature, and matrix inversion. We will build on open-source libraries developed and used by many scientists. They have the advantage to be broadly verified and thoroughly optimized for computational efficiency.

To test our BEM implementation, we will compare numerical results for special test cases to theoretical work within the SPP. This includes thin-film gradient dynamics models for adaptive (**U. Thiele**), or switchable substrates (**S. Gurevich/A. Heuer**), surfactant-laden drops on finite-support (**D. Peschka**), and phase-field model to describe dynamic wetting (**A. Voigt**).

2. Moving and deforming droplets using dynamic wettability patterns

a) moving droplets:
For the first part of this objective we will study simple techniques to move a single droplet forward. At its center is the link between droplet speed and the spatio-temporal properties of the dynamic wettability patterns. We first test a traveling step-like variation in wettability as displayed schematically in Figs. 1(a) and (b). It will carry the droplet along with itself up to a threshold value for the step velocity. Three questions arise: 1. What is this limiting velocity, where the droplet cannot keep up? 2. How is the droplet deformed at various velocities? 3. Finally, how does the response of the droplet depend on its volume or size? We expect the threshold velocity of the traveling step to depend on multiple factors: droplet viscosity, volume, and equilibrium contact angles on both sides of the wettability step. Furthermore, larger step velocities will plausibly lead to stronger deformations. While at small velocities the droplet will approximately keep a circular contact line, it will gradually deform for increasing velocities to a more complicated shape as a growing part of the droplet will enter the low wettability region, when it travels forward with the wettability step. We will determine the center-of-mass velocity of the droplet and quantify its deformation by higher moments of the mass distribution and by the eccentricity of the contact line. We expect larger droplets to move slower because friction forces grow with the footprint area of the droplet.

Another, more complex wettability pattern is a traveling planar wave carrying the droplet along [displayed schematically in Fig. 1(c)]. Here, further questions arise in addition to what we considered above: 1. How does the wavelength of the planar wave affect droplet

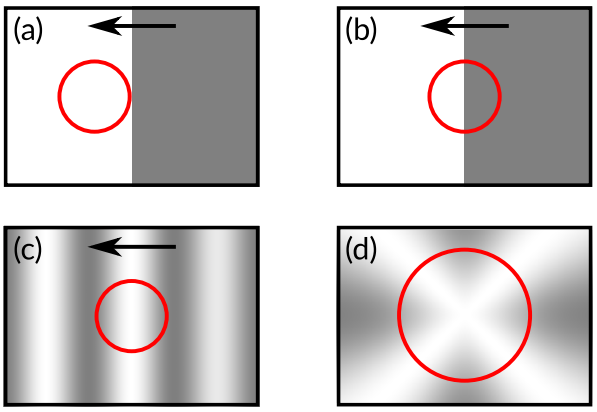

Figure 1: Schematic of droplets (red circles) moving on wettability patterns. Darker shading indicates lower wettability: (a) droplet "pushed" by a slowly moving front, (b) droplet "pushed" by a quickly moving front forcing it to partially cover the less wettable region, (c) droplet pushed by a traveling wave pattern, and (d) droplet in a wettability pattern with harmonic variations along the contact line.

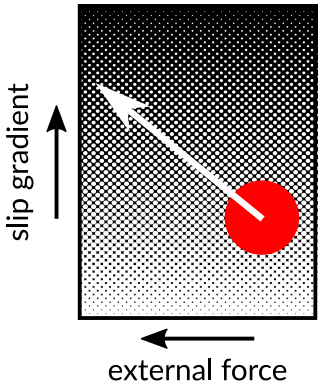

Figure 2: Schematic of a droplet subject to an external force and a gradient in slip length. Darker shading indicates larger slip length. The expected direction of motion is indicated by the arrow.

speed? 2. Since the wave is a repeating pattern, can the droplet may enter an oscillating mode without moving significantly in one direction? 3. Finally, are there specific wave velocities and wavelengths, which maximize droplet speed? Furthermore, the ratio of wavelength to droplet size should be an important quantity. If the wavelength is much larger than the droplet diameter, the variation of wettability along the droplet is small and it hardly moves. For wavelengths smaller than droplet size, we expect the droplet speed and moving direction to depend critically on the size ratio and other parameters such that the droplet moves more irregularly. Potentially, it splits into two smaller droplets, when its central part sits on a low wettability region while the outer parts are tracked into areas with higher wettability. To optimize droplet speed, we expect an optimal wavelength twice the droplet size because it can accommodate the droplet in its high wettability regions, and an optimal wave velocity above the optimal value for the step-like pattern because the repeating pattern of the plane wave can recapture the droplet even if it cannot always keep up with the traveling pattern.

b) deforming droplets:

The second part of this objective aims at a detailed understanding of droplet deformation in response to more complex changes in wettability. We plan to test wettability patterns with harmonic variations along the contact line and two ways of temporal changes, where we either rotate the patterns or oscillate their intensity in place. For example, the "windmill" pattern displayed schematically in Fig. 1(d) is given in polar coordinates by the function $f(r,\varphi) = [1-\exp(-r^2)]\cdot[1+\cos(4\varphi)]$. Such patterns are experimentally realized using Laguerre-Gaussian light modes [68, 69]. We expect the center of mass of the droplet to stay at rest or simply oscillate around a fixed position (due to symmetry) while both its mass distribution and contact line will show complex spatio-temporal variations. To rationalize our observations, we will study several aspects: 1. How is the contact line deformed for various wettability patterns? 2. How does the droplet react to different oscillation frequencies? 3. And what fluid flow is induced inside the droplet? For example, the droplet should be less susceptible to high-frequency oscillations due to internal friction. Furthermore, we expect the contact line to track the harmonic variation prescribed by the wettability pattern and form protrusions into the high wettability regions. Given the fact that some studies have found transitions of the internal flow field between a single vortex and multiple vortices depending on the contact angle [34], we expect complicated flow patterns to emerge in the protruding parts of the droplet. Finally, can we apply our findings to enhance the drift speed of the

droplet discussed in a) by constructing more effective wettability patterns based on our findings in this part? For example, a droplet may move faster if the low wettability region covers the droplet, except for a small region in which the droplet is pushed.

Both studies in part a) and b) require a specific implementation of the BEM, which includes: Firstly, a description of the wall-side and free surfaces of the droplet with their respective boundary conditions. Secondly, a description of the *dynamics* of the free surface in response to the internal flow field of the droplet. Thirdly, a description of the contact line dynamics in response to changing wettability patterns. Together, the dynamics of the free surface, the contact line, and the internal flow field determine droplet motion and deformation. We implement such a BEM as described under the first objective.

It is planned that the project of **R. Haag** provides us with realistic values of dynamic contact angles, while the microscopic investigations of **E. Backus/M. Bonn** provide information about the molecular level details of the solid-gas and gas-liquid interface, which can be related to the substrate surface tensions γ_{sg} and γ_{sl}. The project of **S. Santer** can explicitly generate dynamic wettability patterns using either thin photosensitive polymer films or arrays of photosensitive pillars. We will intensely discuss how to model and thereby understand the experimental results with our BEM program.

3. Driving condensing and evaporating droplets

During condensation molecules move from the oversaturated gas to the liquid phase and the volume of the liquid grows, while during evaporation they leave the liquid and the liquid volume shrinks. To mimic these processes, we can include growth or decay terms, $\pm a\boldsymbol{n}$ with rate a, in the dynamics of the free surface introduced in Eq. (6). Here, we plan to study the combined effect of dynamic wettability patterns and condensation or evaporation on the overall dynamics of a droplet.

As a natural extension of the work in the previous part, we will address the following questions: 1. How does a changing volume affects the response of the droplet to oscillations in the wettability? 2. How does it affects flow inside the droplet? 3. And what happens, in particular, when the rate of volume change and the oscillation frequency of the wettability pattern approach each other? To address these questions, we study droplets with varying rates a of volume change (both positive and negative) and focus especially on the wettability patterns from the previous study, which induce droplet deformations. In addition, we will also vary specific properties of the wettability patterns, which we select based on our earlier findings. Since both the rate of volume change and the frequency of the pattern oscillations couple to the internal degrees of freedom of the droplet, we expect an interesting dynamics when they approach each other.

Evaporating droplets form vortices for small contact angles [34]. They are particular useful for the deposition of solutes and ultimately for use in printing devices. So we will carefully study how the interplay of evaporation and droplet oscillations determines the internal flow field. By carefully choosing the parameters can we control the extension and number of vortices and thereby purposefully deposit a solute while the droplet is drying.

4. External forces acting on driven droplets

In this part we will combine the response to spatio-temporal wettability patterns with the presence of external forces, such as gravity or the electrostatic forces. They modify the contact angle of the droplet because as body forces they act on the whole droplet and thereby alter its shape, while without external forces, the shape of the free surface (in static equilibrium) is only determined by minimizing the total surface energy. For a uniform distribution of mass or an ideally conducting droplet liquid this study can be performed using BEM, because the respective forces can be calculated purely by their effect on the droplet boundaries. For example, to include gravitational forces with acceleration $\boldsymbol{g}$ for a fluid with

constant density ρ, one adds $\rho \boldsymbol{g} \cdot \boldsymbol{r}$ to the pressure, which adds an additional stress term $(\rho \boldsymbol{g} \cdot \boldsymbol{r})\boldsymbol{n}$ to the boundary conditions for $\boldsymbol{\Sigma n}$ mentioned in Sec. 1.0.2 [45]. For a conducting droplet liquid, where an electric field acts across the substrate from a charged plate below it to the droplet footprint, one has to add the Maxwell stress tensor to $\boldsymbol{\Sigma}$.

We will apply the wettability patterns for moving and deforming a droplet introduced in the second objective and test if external forces, which act normal to the substrate, enhance or suppress droplet motion and deformation. For example, when gravity presses the droplet fluid onto the substrate, the area of the footprint of the droplet increases and thereby its friction. Of interest is also how a non-wetting droplet behaves with parts of its free surface hanging above the non-wetted substrate. The gravitational force stays constant in time, while we will also apply oscillating electric fields. It will be interesting to observe, how the droplet reacts on the combined action of the dynamic wettability pattern and an applied oscillating electric field. If their frequencies are incommensurate, we expect irregular dynamics, which needs to be analyzed. This might provide an interesting method for mixing fluids at low Reynolds number.

We will proceed by investigating external forces with a component along the substrate. For example, this is realized by gravity acting on a droplet on an inclined surface. Specifically, we will study a planar wave wettability pattern traveling up the inclined substrate and ask how effective it is to compensate the downward directed gravitational force in order to stop the droplet. For static wettability patterns, sufficiently large gradients in wettability were shown to overcome gravity [7].

5. Dynamic wetting on rough substrates

The BEM, which we will implement according to the theory presented in Sec. 1.0.2, also implements the Navier condition at the liquid/substrate interface. The boundary condition also contains a possibly non-zero slip length, which allows the liquid to slip over the substrate with a non-zero velocity. Typically, this occurs on rough surfaces. The project of **R. Haag** will explicitly fabricate substrates with a surface roughness by coating them with a polymer layer. Comparing experimental contact angles to theoretical predictions, where we vary the slip length, will not only clarify if a non-zero slip length can describe the wetting behavior of the polymer coatings but it will also help to measure these slip lengths.

Furthermore, we will also investigate whether and how a gradient in slip length influences directed motion of the droplet, *e.g.*, due to gravity. Because larger slip lengths permit faster motion of the contact line, the mobility of the droplet increases. If one part of the contact line moves faster than the rest, the droplet deforms and develops an anisotropic friction coefficient. For a driving force perpendicular to the slip gradient, the droplet also develops a drift motion perpendicular to the force and we expect it to move at an angle to the force direction (see schematic in Fig. 2). A related, open question is whether a slip gradient induces droplet motion due to an internal flow field of the droplet, which is, *e.g.*, induced by shaking the droplet with an oscillating electric field.

Long-term perspective: Collective dynamics of droplets on switchable substrates

One long-term perspective is to extend our study to the dynamics of multiple droplets on light-switchable substrates. As noted earlier, control of droplet size is crucial in many technical applications, including printing and cooling devices. Therefore, we are specifically interested to investigate how the dynamics of splitting and merging droplets can be influenced and controlled by dynamic wettability patterns. Extending our BEM code to treat multiple droplets will pose a challenge.

Some related cases have already been studied. For example, Asgari *et al.* identified static wettability patterns speeding up the merging of two droplets while others slowed it down [26]. Relatedly, Kaspar *et al.* demonstrated in simulations and experiments that

a static checkerboard pattern can effectively form and confine many droplets of a specific size at the same time [12]. Finally, Seki *et al.* developed a theory for droplets sitting on a light-sensitive liquid crystal, which explains how droplets accumulate locally in response to light [70]; a phenomenon observed in earlier experiments [71]. These findings inspire us to strive for a deeper understanding of the collective dynamics of droplets on switchable substrates.

Work schedule

We will first complete the work on implementing the BEM during ca. 6 months of the first year and extend it thereafter as required by the project. We will then work on moving and deforming droplets by dynamic wettability patterns for ca. one year. This is followed by taking into account evaporation and condensation of the water droplets, which will take ca. 0.75 year and the influence of external forces will be studied in the last 0.75 year. In parallel we will look at dynamic wetting on rough surfaces as required by the project of **R. Haag** (FU Berlin) and be open to problems of other groups coming up during work within the SPP.

2.4 Data handling

The numerical data produced during the simulations will be stored on standard hard disks. All data, relevant to published work, as well as source codes are stored in the version control system and the data backup system of the *TUBIT* (*Technische Universität Berlin*, I.T. services).

Sections 2.5 - 2.7 Do not apply

2.8 Information on scientific cooperation within SPP 2171

The project proposal is situated right in the center of the priority program. Its main research idea, which investigates how dynamic wettability patterns drive droplets sitting on a substrate out of equilibrium, addresses one of the key areas of the priority program, namely switchable substrates. Thereby, it provides a fundamental understanding of the underlying physical processes and lays the ground for future applications in cooling or dehumidification devices, and in printing technologies. The BEM, which we develop in the beginning, is a versatile tool. It has the potential to be extended to flexible and adaptive surfaces, the other key areas of the priority program. Thereby, it not only supports experimental projects on switchable substrates but appropriately modified may also address dynamic wetting on the other types of substrates.

Experiments:
As already mentioned we will have a collaboration with **R. Haag** on dynamic wetting on (photo-)switchable and rough substrates and with **E. Backus/M. Bonn**, who measure microscopic details during photo-switching. In particular, both groups will provide realistic parameters (dynamic contact angles and surface tensions) for our theoretical modelling. We will also collaborate with **S. Santer**, who plans to generate dynamic wettability patterns using various types of photosensitive substrates.

There are further projects dealing with photo-switchable substrates, namely from **S. Gorb**, **O. Lieleg**, and **C. Collfrank**, where photo-stimulated switches are used in order to generate an anisotropic adaptive surface and from **R. Stannarius**, which investigates wetting of

optically switchable anisotropic surfaces. In the course of the ongoing work in the SPP, we are open to explore if and how we can address these specific systems.

Theory:
We will collaborate with the project of **S. Gurevich/A. Heuer**, who also work on switchable substrates mainly uniform or with stripe geometries. They use complementary methods ranging from microscopic theories to thin-film equations. We will identify special test cases in order to compare our methods.

Furthermore, we will have a methodological exchange with **A. Reusken** on the comparison of the finite-element method with the BEM used in our project, and with **A. Voigt**, who uses a phase-field model to describe dynamic wetting.

To foster the exchange between theoretical groups working with continuum-theoretical approaches within the SPP, we have initiated an informal network, which includes the groups of **M. Brinkmann**, **S. Gurevich**, **D. Peschka**, **J. Snoeijer**, **H. Stark**, **U. Thiele**, **A. Voigt**, and **B. Wagner**, and which is open to others. There, we will coordinate aspects of the training of the involved young researchers within the SPP and meet sporadically to discuss details of our approaches and ongoing work.

Finally, we will familiarize other groups within the SPP with our BEM program by formulating hands-on tutorials, where the young researchers have the opportunity to learn about the BEM program.

3 Bibliography

[1] G. Lagubeau, M. L. Merrer, C. Clanet, and D. Quéré, Nat. Phys. **7**, 395 (2011).

[2] A. Wixforth, Superlattices Microstruct. **33**, 389 (2003).

[3] K. Ichimura, S. Oh, and M. Nakagawa, Science **288**, 1624 (2000).

[4] M. Chen, Z. Jia, T. Zhang, and Y. Fei, Appl. Surf. Sci. **433**, 336 (2018).

[5] B. Gątarski and W. Nowicki, Surf. Innov. **5**, 170 (2017).

[6] X. Wang, S. Zhang, C. Guo, and Z. Yuan, Nano **10**, 1550051 (2015).

[7] M. K. Chaudhury and G. M. Whitesides, Science **256**, 1539 (1992).

[8] G. Karapetsas, N. T. Chamakos, and A. G. Papathanasiou, Langmuir **33**, 10838 (2017).

[9] J. Won, W. Leet, and S. Song, Sci. Rep. **7**, 3062 (2017).

[10] H. P. Greenspan, J. Fluid. Mech. **84**, 125 (1978).

[11] T. Ondarçuhu and M. Veyssié, J. Phys. II **1**, 75 (1991).

[12] O. Kašpar, H. Zhang, V. Tokárová, R. I. Boysen, G. R. Suñé, X. Borrise, F. Perez-Murano, M. T. W. Hearn, and D. V. Nicolau, Lab Chip **16**, 2487 (2016).

[13] C. Lv and P. Hao, Langmuir **28**, 16958 (2012).

[14] C. Liu, J. Sun, J. Li, C. Xiang, L. Che, Z. Wang, and X. Zhou, Sci. Rep. **7**, 7552 (2017).

[15] D. Bonn, J. Eggers, J. Indekeu, J. Meunier, and E. Rolley, Rev. Mod. Phys. **81**, 739 (2009).

[16] K. B. Glasner, J. Comp. Phys. **207**, 529 (2005).

[17] L. Makkonen, J. Chem. Phys. **147**, 064703 (2017).

[18] F. Brochard, Langmuir **5**, 432 (1989).

[19] R. S. Subramanian, N. Moumen, and J. B. McLaughlin, Langmuir **21**, 11844 (2005).

[20] Q. Liu and B. Xu, Extrem. Mech. Lett. **9**, 304 (2016).

[21] A. Oron, S. H. Davis, and S. G. Bankoff, Rev. Mod. Phys. **69**, 931 (1997).

[22] A. Moosavi and A. Mohammadi, J. Phys.: Condens. Matter **23**, 085004 (2011).

[23] T. Liu, N. Nadermann, Z. He, S. H. Strogatz, C. Hui, and A. Jagota, Langmuir **33**, 4942 (2017).

[24] L. W. Schwarz and R. R. Eley, J. Colloid Interface Sci. **202**, 173 (1998).

[25] M. Sellier, Ph.D. thesis, University of Leeds (2003).

[26] M. Asgari and A. Moosavi, Phys. Rev. E **86**, 016303 (2012).

[27] C. Huh and L. E. Scriven, J. Colloid Interface Sci. **35**, 85 (1971).

[28] B. C. Bunker, Mater. Sci. Eng. R **62**, 157 (2008).

[29] D. Baigl, Lab Chip **12**, 3637 (2012).

[30] J. Berná, D. A. Leigh, M. Lubomska, S. M. Mendoza, E. M. Pérez, P. Rudolf, G. Teobaldi, and F. Zerbetto, Nat. Mater. **4**, 704 (2005).

[31] D. Yang, M. Piech, N. S. Bell, D. Gust, S. Vail, A. A. Garcia, J. Schneider, C. Park, M. A. Hayes, and S. T. Picraux, Langmuir **23**, 10864 (2007).

[32] H. Y. Erbil, Adv. Colloid Interface Sci. **170**, 67 (2012).

[33] M. Edalatpour, L. Liu, A. Jacobi, K. Eid, and A. Sommers, Appl. Energy **222**, 967 (2018).

[34] H. Gelderblom, O. Bloemen, and J. H. Snoeijer, J. Fluid Mech. **709**, 69 (2012).

[35] S. N. Varanakkottu, M. Anyfantakis, M. Morel, S. Rudiuk, and D. Baigl, Nano Lett. **16**, 644 (2016).

[36] M. Alwazzan, K. Egab, B. Peng, J. Khan, and C. Li, Int. J. Heat Mass Transf. **112**, 991 (2017).

[37] R. D. Deegan, O. Bakajin, T. F. Dupont, G. Huber, S. R. Nagel, and T. A. Witten, Nature **389**, 827 (1997).

[38] H. Hu and R. G. Larson, J. Phys. Chem. B Lett. **110**, 7090 (2006).

[39] B. M. Weon and J. H. Je, Phys. Rev. E **82**, 015305(R) (2010).

[40] P. J. Yunker, T. Still, M. A. Lohr, and A. G. Yodh, Nature **476**, 308 (2011).

[41] Y. Li, Y. Sheng, and H. Tsao, Langmuir **29**, 7802 (2013).

[42] U. Thiele, M. G. Velarde, K. Neuffer, M. Bestehorn, and Y. Pomeau, Phys. Rev. E **64**, 061601 (2001).

[43] U. Thiele, K. Neuffer, M. Bestehorn, Y. Pomeau, and M. G. Velarde, Colloids Surf. A **206**, 87 (2002).

[44] F. Mugele, A. Klingner, J. Buehrle, D. Steinhauser, and S. Herminghaus, J. Phys.: Condens. Matter **17**, S559 (2005).

[45] C. Pozrikidis, *Boundary integral and singularity methods for linearized viscous flow* (Cambridge University Press, Cambridge, 1992).

[46] C. Pozrikidis, J. Comp. Phys. **169**, 250 (2001).

[47] E. Alinovi and A. Bottaro, J. Comp. Phys. **356**, 261 (2017).

[48] *QuadGK.jl* (2018), `https://github.com/juliamath/QuadGK.jl/`.

[49] A. Zöttl and H. Stark, J. Phys.: Condens. Matter **28**, 253001 (2016).

[50] R. Tavarone, P. Charbonneau, and H. Stark, J. Chem. Phys. **144**, 104703 (2016).

[51] M. Schmitt and H. Stark, Phys. Fluids **28**, 012106 (2016).

[52] J. Grawitter and H. Stark, Soft Matter **14**, 1856 (2018).

[53] E. Chevallier, A. Mamane, H. A. Stone, C. Tribet, F. Lequeux, and C. Monteux, Soft Matter **7**, 7866 (2011).

[54] M. Schmitt and H. Stark, Europhys. Lett. **101**, 44008 (2013).

[55] M. Schmitt and H. Stark, Eur. Phys. J. E **39**, 80 (2016).

[56] S. Kaneko, K. Asakura, and T. Banno, Chem. Commun. **53**, 2237 (2017).

[57] Y. Xiao, S. Zarghami, K. Wagner, P. W. K. C. Gordon, L. F. D. Diamond, and D. L. Officer, Adv. Mater. p. 1801821 (2018).

[58] S. Kim and S. J. Karrila, *Microhydrodynamics* (Dover Publications, Mineola/NY, 2005).

[59] C. Pozrikidis, *A practical guide to boundary element methods with software library BEMLIB* (CRC Press, Boca Raton/FL, 2002).

[60] H. B. Eral, D. J. C. M. 't Mannetje, and J. M. Oh, Colloid Polym. Sci. **291**, 247 (2013).

[61] R. Ledesma-Aguilar, A. Hernández-Machado, and I. Pagonabarraga, Phys. Rev. Lett. **110**, 264502 (2013).

[62] J. H. Snoeijer and B. Andreotti, Annu. Rev. Fluid Mech. **45**, 269 (2013).

[63] O. V. Voinov, Fluid Dyn. **11**, 714 (1976).

[64] R. G. Cox, J. Fluid Mech. **168**, 169 (1986).

[65] I. Bajlekov, Ph.D. thesis, Technische Universiteit Eindhoven (2003).

[66] I. B. Bazhlekov, P. D. Anderson, and H. E. H. Meijer, Phys. Fluids **16**, 1064 (2004).

[67] *BEMLIB* (2016), version 16.07 (accessed 2018-07-17), `http://dehesa.freeshell.org/BEMLIB/`.

[68] L. Allen, M. W. Beijersbergen, R. J. C. Spreeuw, and J. P. Woerdman, Phys. Rev. A **45**, 8185 (1992).

[69] M. Padgett and R. Bowman, Nat. Photonics **5**, 343 (2011).

[70] K. Seki and M. Tachiya, J. Phys.: Condens. Matter **17**, S4229 (2005).

[71] T. Yamamoto, J. Yamamoto, B. I. Lev, and H. Yokoyama, Appl. Phys. Lett. **81**, 2187 (2002).

4 Requested modules/funds

4.1 Funding for staff

4.1.1 Research staff

4.1.1.1 Non-doctoral staff:
Funds are requested for the period of 36 months to pay a Ph.D. student according to the salary scale 75 % TV-Berlin E13. Josua Grawitter, an excellent student, has initiated the proposed research and already performed initial work on the project. It is planned that he finishes his thesis on the project and then hands over to his successor.

4.1.1.2 Postdoctoral staff: no request

4.1.1.3 Other research assistants: no request

4.1.2 Non-academic staff

no request

4.1.3 Student assistants

no request

4.2 Funding for direct project costs

4.2.1 Equipment up to 10,000 EUR, software and consumables

no request

4.2.2 Travel

In total we request travel funds of 13,900 EUR. They are justified as follows.

a) The results of our research should be presented on the spring meeting of the *Deutsche Physikalische Gesellschaft* in the years 2020, 2021, and 2022. For three meetings for two researchers (the doctoral researcher and the applicant) $3 \times 2 \times 600$ EUR = 3,600 EUR are needed.

b) The results should also be presented on an international conference, for example, the March meeting of the *American Physical Society* in the years 2020, 2021, and 2022 either by the applicant or the doctoral researcher.

   For one conference visit the following costs arise: travel costs: ca. 700 EUR, conference fee ca. 250 EUR, costs for accommodation and food during the conference visit of ca. 750 EUR, which gives a total of 1,700 EUR.

   For three conference visits, this amounts to a total of 5,100 EUR.

c) For visits to cooperating groups within the priority program, we estimate 300 EUR per year. For three years, this amounts to a total of 900 EUR.

d) For SPP events a total of 4,300 EUR are requested:
   – 1st and 2nd year: workshop (4 days) attended by applicant and Ph.D. student: $2 \times 2 \times 500$ EUR = 2,000 EUR
   – 1st year: Advanced School for Ph.D. students (5 days): 600 EUR
   – 2nd year: Ph.D.-candidate workshop (4 days): 500 EUR
   – 3rd year: International conference (5 days) attended by applicant and Ph.D. student: 2×600 EUR = 1,200 EUR

4.2.3 Visiting researchers

no request

4.2.4 Experimental animals

no request

4.2.5 Other

no request

4.2.6 Project-related publication expenses

For the publication of our scientific results within the project 2250 EUR are requested for three years.

4.3 Funding for instrumentation

no request

5 Project requirements

5.1 Employment status information

Prof. Dr. Holger Stark, professor for Theoretical Physics, *Technische Universität Berlin*, permanent position

5.2 First-time proposal data

Does not apply

5.3 Composition of the project group

The applicant is professor for theoretical physics at *TU Berlin* and works on the statistical physics of soft matter and biological systems. His general interests are hydrodynamic problems in both areas.

Several of the applicant's team members will contribute to the proposed project with their expertise on hydrodynamic flow problems at low Reynolds numbers: Dr. Jérôme Burelbach (funded by TU Berlin) contributes his fundamental understanding of hydrodynamics, Arne Zantop (funded by TU Berlin) and Christian Schaaf (funded by SFB 910) provide support on the numerical work, and Reinier van Buel (funded by SFB 910), who works on visco-elastic fluids, gives advice on interpreting the results. Our secretary, Heike Klemz, will be available for administrative work.

5.4 Cooperation with other researchers

5.4.1 Researchers with whom you have agreed to cooperate on this project

See Sec. 2.8

5.4.2 Researchers with whom you have collaborated scientifically within the past three years

The applicant has collaborated on joint scientific projects within the past three years with Dr. Adhyapak (Mainz), Prof. Babu (ITT Delhi), Dr. Blaschke (Berkeley), Prof. Beta (Potsdam), Prof. Biais (Brooklyn College), Prof. Charbonneau (Duke University), Prof. Ejtehadi (Tehran), Prof. Engstler (Würzburg), Dr. Gurevich (Berlin), Prof. Kapral (Toronto), Dr. Malgaretti (Stuttgart), Prof. Pototsky (Hawthorn, Australia), Prof. Schmiedeberg (Erlangen), Prof. Thiele (Münster), Prof. Zaburdaev (Erlangen), and Dr. Zöttl (Vienna).

5.5 Scientific equipment

The *Institut für Theoretische Physik* runs a cluster of state-of-the-art personal computers, which will be used for developing computer codes within the project. For extended simulations, a computer cluster in the computing center of the *Faculty II, Mathematics and Natural Sciences*, is available.

Sections 5.6 and 5.7 Do not apply

6 Additional information Does not apply